

Multimodal Imaging of Optic Nerve Head in Retinitis Pigmentosa

Naoko Wada, Seiji Takagi, Akiko Yoshikawa, Takashi Itokawa, Takahiro Maruyama & Yuichi Hori

To cite this article: Naoko Wada, Seiji Takagi, Akiko Yoshikawa, Takashi Itokawa, Takahiro Maruyama & Yuichi Hori (08 Jun 2024): Multimodal Imaging of Optic Nerve Head in Retinitis Pigmentosa, Seminars in Ophthalmology, DOI: [10.1080/08820538.2024.2363849](https://doi.org/10.1080/08820538.2024.2363849)

To link to this article: <https://doi.org/10.1080/08820538.2024.2363849>



© 2024 The Author(s). Published with license by Taylor & Francis Group, LLC.



Published online: 08 Jun 2024.



Submit your article to this journal [↗](#)



Article views: 59



View related articles [↗](#)



View Crossmark data [↗](#)

Multimodal Imaging of Optic Nerve Head in Retinitis Pigmentosa

Naoko Wada^a, Seiji Takagi^a, Akiko Yoshikawa^a, Takashi Itokawa^a, Takahiro Maruyama^{a,b}, and Yuichi Hori^a

^aDepartment of Ophthalmology, School of Medicine, Toho University, Tokyo, Japan; ^bDepartment of Ophthalmology, Tokyo Shinagawa Hospital, Tokyo, Japan

ABSTRACT

Background: A pallor optic nerve head (ONH) is one of the three features of retinitis pigmentosa (RP). This study aimed to assess the ONH prospectively by color tone, presence of hyper-reflective tissue, blood flow, retinal nerve fiber layer (RNFL) thickness, ganglion cell complex (GCC) and investigate the change in these parameters with and without ONH pallor.

Methods: The presence of ONH pallor was assessed by three independent examiners through careful examination using fundus photographs. The presence of a hyper-reflective structure on the ONH was carefully evaluated using a volume scan optical coherence tomography (OCT). RNFL thickness and ellipsoid zone (EZ) width around the macula were also evaluated by OCT. Laser speckle flowgraphy was used to measure the mean blur rate of the entire ONH area, which was subsequently divided into the vessel area (MV) and tissue area (MT).

Results: Twenty-eight eyes of 28 patients with RP (55.4 ± 16.23 years of age) were included. The pale ONH was observed in 10 (35%) eyes. Hyper-reflective structures were observed in seven (25%) eyes. No significant correlation was found between the pale ONH and the presence of a hyper-reflective structure (Pearson's chi-squared test, $p = .364$). The average of the ONH area, MV, and MT was 8.65 ± 3.08 AU, 17.81 ± 7.54 AU, and 6.4 ± 2.66 AU, respectively, which significantly decreased in patients with pallor ONH (all $p < .05$). The global RNFL thickness was $73.54 \pm 18.82 \mu\text{m}$. The nasal and superior quadrants and global RNFL thickness in patients with a pale ONH were significantly thinner than in patients without a pale ONH (all $p < .05$). The global and superior and inferior GCC thickness in patients with a pale ONH were significantly thinner than in patients without a pale ONH (all $p < .05$). There was no difference in the EZ width between patients with and without a pale ONH ($p = .107$).

Conclusion: We conducted multiple assessments of the ONH in RP patients and investigated its clinical significance. Our findings suggest that ONH pallor may indicate a comprehensive change that emerges alongside the progression of retinal degeneration in RP.

Trial registration: This trial was retrospectively registered in the UMIN Clinical Trial Registry (UMIN ID: 000048168).

ARTICLE HISTORY

Received 8 April 2024

Revised 25 May 2024

Accepted 30 May 2024

KEYWORDS

Blood flow; laser speckle flowgraphy; optic nerve head; optical coherence tomography; pallor optic disc; prelaminar membrane; retinal nerve fiber layer; retinitis pigmentosa

INTRODUCTION

Retinitis pigmentosa (RP), a clinically and genetically heterogeneous disease, is the most commonly inherited retinal dystrophy and a major cause of blindness and visual handicap in the developed world.^{1,2} There has been no effective treatment for RP, but in recent years, several treatments have been intensively studied, including gene therapy,³ cell transplantation therapy,⁴ and retinal prostheses.⁵ Since these therapies are based on the recovery of photic stimulus input as the first neuron, the health of second-order neurons and beyond is the key to achieving the treatment scheme. Therefore, an accurate assessment of the residual neurotic function in patients would determine the therapeutic effect in clinical practice.

One of the triad findings of RP is the waxy pallor presentation of the optic nerve head (ONH). It has been reported that the color of ONH is normal in the early stage and appears waxy and pale in the advanced stage.⁶ Studies have reported that the epiretinal membrane on the ONH, which is formed as degeneration progresses, causes this color change,⁷ and recently the presence of membrane-like tissue in RP was evaluated by optical coherence tomography (OCT).

Furthermore, studies have demonstrated that RP patients with pallor ONH exhibit thinner retinal nerve fiber layers (RNFL) than those without pallor ONH.⁸ However, the clinical implications of these findings have not been fully investigated. Significant advancements in ocular imaging technology have drawn considerable attention to changes in the vascularity of the RP. Laser speckle flowgraphy (LSFG) can quantitatively estimate the blood flow in a clinical setting.⁹

This study aimed to assess the color tone of the ONH, examine the morphological changes in and around the ONH, and evaluate the blood supply to the ONH in patients with RP. Furthermore, these findings were compared between patients with and without pallor.

MATERIALS AND METHODS

Study Design

This prospective study adhered to the principles of the Declaration of Helsinki and was approved by the ethics committee of the Toho University Omori Medical Center (approval number: M20053). All participating patients

provided informed consent to participate in this observational study. This study was retrospectively registered in the UMIN Clinical Trial Registry (UMIN ID:000048168).

Patients

This cross-sectional observational study included consecutive patients with RP who were admitted to the Retinal Degeneration Outpatient Department of Toho University Medical Center Omori Hospital between September 2020 and September 2022. Patients were diagnosed with RP based on their clinical history, fundus appearance, visual field assessments, and full-field electroretinogram findings according to the guidelines of the Japanese Ophthalmological Society.

At the initial visit after enrolment, all patients underwent complete ocular examinations, including spherical equivalent (SE), best-corrected visual acuity (BCVA), intraocular pressure, slit-lamp biomicroscopy, dilated funduscopy, fundus photography, OCT, and LSFG measurements. BCVA was obtained using Landolt C-charts and was subsequently converted to the logarithm of the minimum angle of resolution (logMAR) for statistical comparisons.

Exclusion criteria were poor LSFG image quality, refractive errors below -6 diopters or above $+3$ diopters, and other potentially confounding retinal pathologies, including glaucoma and neuro-ophthalmological diseases. Patients with cystoid macular edema, posterior subcapsular cataract, or epiretinal membrane were also excluded to ensure appropriate evaluation of the ONH color. The genetic characterization and mode of inheritance were beyond the scope of this study. If both eyes of a patient were available, only the right eye of the patient was selected and included in the analysis because of the high correlation observed between both eyes.

Multimodal Imaging of ONH

All images were captured under mydriasis, which was obtained by applying 0.5% tropicamide and 0.5% phenylephrine (Santen, Osaka, Japan) before the inspection.

Figure 1 shows the multimodal imaging of the ONH in RP using fundus photographs, OCT imaging, and LSFG map.

Fundus Photo and WAXY Pallor of the ONH

Color fundus photographs centered on the macula and ONH were obtained using a digital fundus camera (ImageNet; Topcon Corp., Tokyo, Japan). The ONH was independently assessed as pale or not pale by three well-trained senior ophthalmologists, including two retina specialists (ST and SK) and one glaucoma specialist (TT). The presence or absence of pallor was assessed with an agreement of at least two out of three evaluators. Patients with cataracts or intermediate translucency that could affect the color of the fundus photographs were excluded.

RNFL and Ganglion Cell Complex (GCC) Analysis Using a Spectral-Domain OCT (SD-OCT)

RNFL measurements were performed using an SD-OCT (RS3000, NIDEK, JAPAN) instrument, with the following

settings: 53000 A-scans per second, $20^\circ \times 20^\circ$ field (approximately 6×6 mm area). A confocal scanning laser ophthalmoscope was used for imaging. RNFL thickness was measured within a circular area with a diameter of 3.45 mm around the ONH center. The software in the device calculates the parameters. The average thickness of this zone corresponds to the global peripapillary RNFL thickness and includes the nasal, temporal, superior, and inferior quadrants of the RNFL.

GCC measurements were also performed using the same instrument, with a 9×9 -mm area. The average thickness of this zone corresponds to the global GCC thickness and includes the superior and inferior quadrants of the GCC.

Presence of a Membrane on the ONH and Ellipsoid Zone (EZ) Width

SD-OCT images (Spectralis; Heidelberg Engineering, Germany) were used to analyze the ONH and macula. Volume scans (a series of raster scans) centered on the ONH were performed, which comprised 40,000 A-scans for each eye. A series of 25 laser scans in a $20^\circ \times 20^\circ$ field (approximately 6×6 mm area) was acquired. The presence of a membrane on the ONH was evaluated and independently graded by three ophthalmologists. The membrane was characterized by a thick, hyper-reflective structure, but it was difficult to distinguish whether it was in the posterior vitreous membrane or not.

The EZ width was manually measured at the fovea using an internal measuring software. The EZ width was defined as the distance between the temporal and nasal borders on the horizontal image of the EZ where the EZ line disappeared.

LSFG

LSFG-NAVI™ (Softcare Co., Fukuoka, Japan) was used to acquire the LSFG images. LSFG is an advanced image analysis method that measures the fundus blood flow using the laser speckle method, wherein a long-wavelength laser (830 nm) is directed toward the fundus, and a random speckle pattern is formed by the reflected scattered light from the blood cells. The blood flow velocity is then calculated based on the rate of change of the pattern.

The mean blur rate (MBR), which is measured in arbitrary units (AU), represents the velocity of blood flow and is obtained by calculating the reciprocal of the square of the contrast of the speckle pattern. The ONH area (MA) was manually delineated by positioning an ellipsoidal region on the ONH margin. The MBR can be determined using the entire MA, and then the LSFG software automatically subdivides the ONH area into the vessel area (MV) and tissue area (MT).

Measurement of Other Systemic and Ocular Parameters

Systolic blood pressure (SBP) and diastolic blood pressure (DBP) were measured before performing LSFG. The mean arterial pressure (MAP) was calculated as $DBP + 1/3(SBP - DBP)$. Ocular perfusion pressure was calculated as $2/3MAP - IOP$.

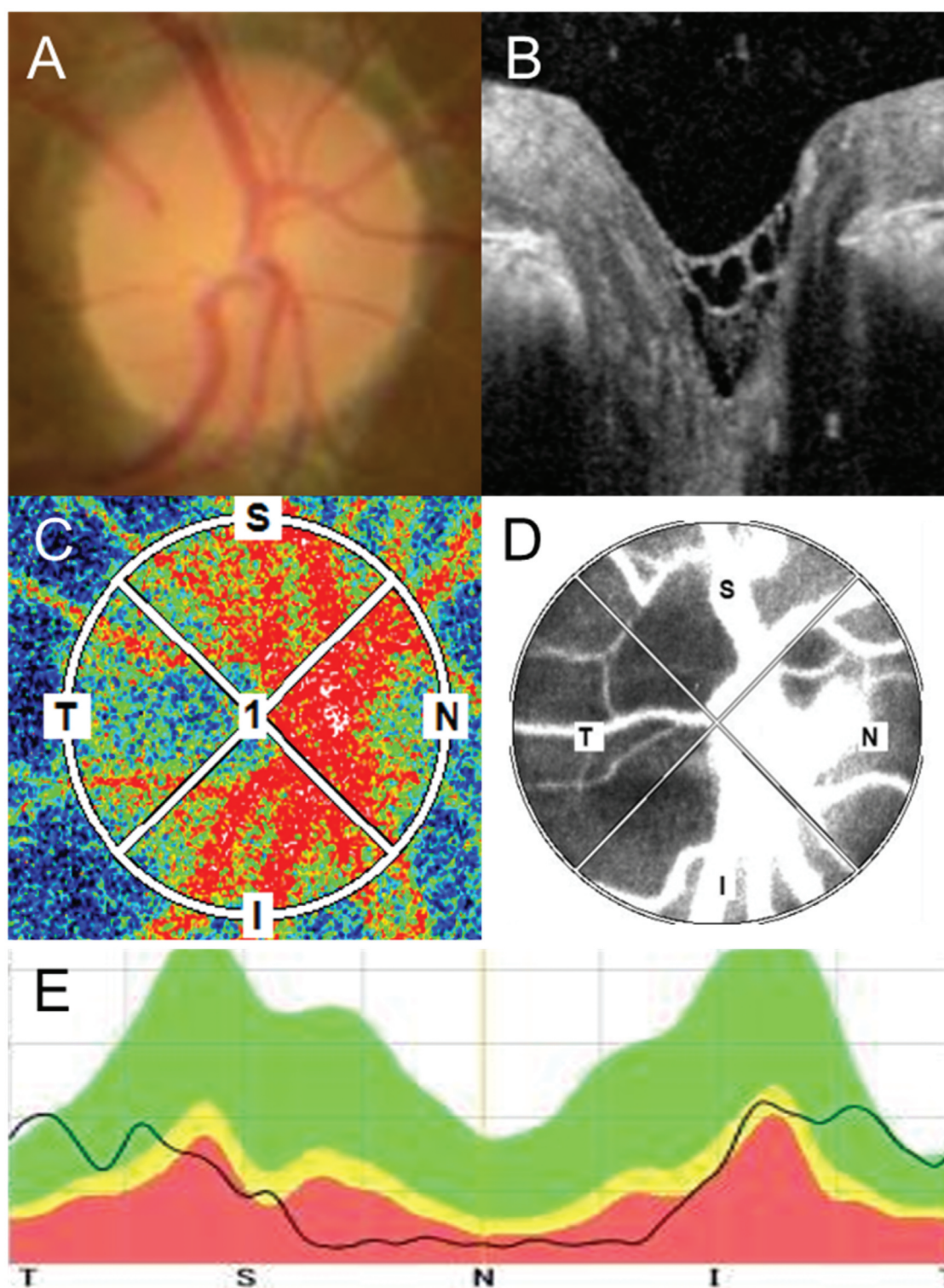


Figure 1. Multimodal imaging of the ONH in RP. (A) The color of the ONH was evaluated using fundus photographs. (B) The presence of a hyper-reflective structure on the ONH was evaluated using 31 volume slices of OCT images. (C) The blood flow was evaluated using LSFG. The colors in the LSFG map represent the average MBR during a single heartbeat. Warmer colors represent a higher MBR, and cooler colors represent a lower MBR. (D) Images were inverted into binary images to evaluate the blood flow in the vessel (white area) and tissue (black area). (E) The thickness of the RNFL was evaluated around the ONH. ONH, optic nerve head; RP, retinitis pigmentosa; OCT, optic coherence tomography; LSFG, laser speckle flowgraphy; MBR, mean blur rate; RNFL, retinal nerve fiber layer.

Statistical Analyses

All statistical analyses were performed using EZR (Saitama Medical Center, Jichi Medical University, Saitama, Japan), which is a graphical user interface for R 2.7–0 (Statistical

Computing, Vienna, Austria) that incorporates functions commonly employed in clinical studies.¹⁰

The results of the descriptive analyses are reported as the mean \pm standard deviation. The Mann–Whitney U test and Spearman's test were used to compare groups with and

without a waxy pale ONH. The relationship between pale ONH and hyper-reflective structure was examined using the chi-squared test. The statistical significance was set at $p < .05$.

RESULTS

We examined 28 of 51 patients (55.4 ± 16.23 years of age, 11 men, 17 women), wherein one eye per patient was included. We excluded 23 eyes because of poor image quality, epiretinal membrane, and cystoid macular edema. All patients were Japanese. The mean logMAR BCVA was 0.28 ± 0.51 . The mean EZ width was 3170 ± 2720 (range, 0 – 8633) μm , and five patients had EZ disruption at the fovea.

The demographics of the patients with RP with and without a pale ONH appearance are shown in Table 1. There was no statistically significant difference between the two groups in age ($p = .125$), male:female ratio (4:6 versus 7:11, respectively, Pearson’s chi-squared test, $p = 1$), SE ($p = .067$), and EZ width ($p = .107$). A significant difference was observed in the BCVA of the patients ($p < .05$).

Table 1. Demographics of the patients with retinitis pigmentosa.

	Pale	Not pale	p-value
N	10	18	
Age (years)	62.9 ± 19.0	52.8 ± 15.0	0.125
Sex (male)	4 (40%)	7 (38%)	
IOP (mmHg)	14.7 ± 2.26	13.38 ± 2.30	0.318
SBP (mmHg)	133 ± 28.55	127 ± 24.4	0.362
DBP (mmHg)	74.7 ± 15.3	79.3 ± 9.76	0.171
OPP (mmHg)	48.2 ± 13.3	50.1 ± 8.65	0.28
MAP (mmHg)	94.0 ± 20.3	95.2 ± 13.2	0.41
SE	-1.57 ± 2.42	-3.49 ± 2.86	0.067
BCVA (logMAR)	0.70 ± 0.68	0.05 ± 0.16	0.000894
EZ width (μm)	2367 ± 2917	3616 ± 2663	0.107

The data are presented as the mean \pm standard deviation. The p-value was calculated using the Mann–Whitney U test, and significance was set at $p < .05$. IOP, intraocular pressure; SBP, systolic blood pressure; DBP, diastolic blood pressure; OPP, ocular perfusion pressure; MAP, mean arterial pressure; SE, spherical equivalent; BCVA, best-corrected visual acuity; logMAR, logarithm of the minimum angle of resolution; EZ, ellipsoid zone.

Figure 2 shows representative ONH of RP patients with and without waxy pallor appearance of the ONH and with and without a hyper-reflective structure on the ONH.

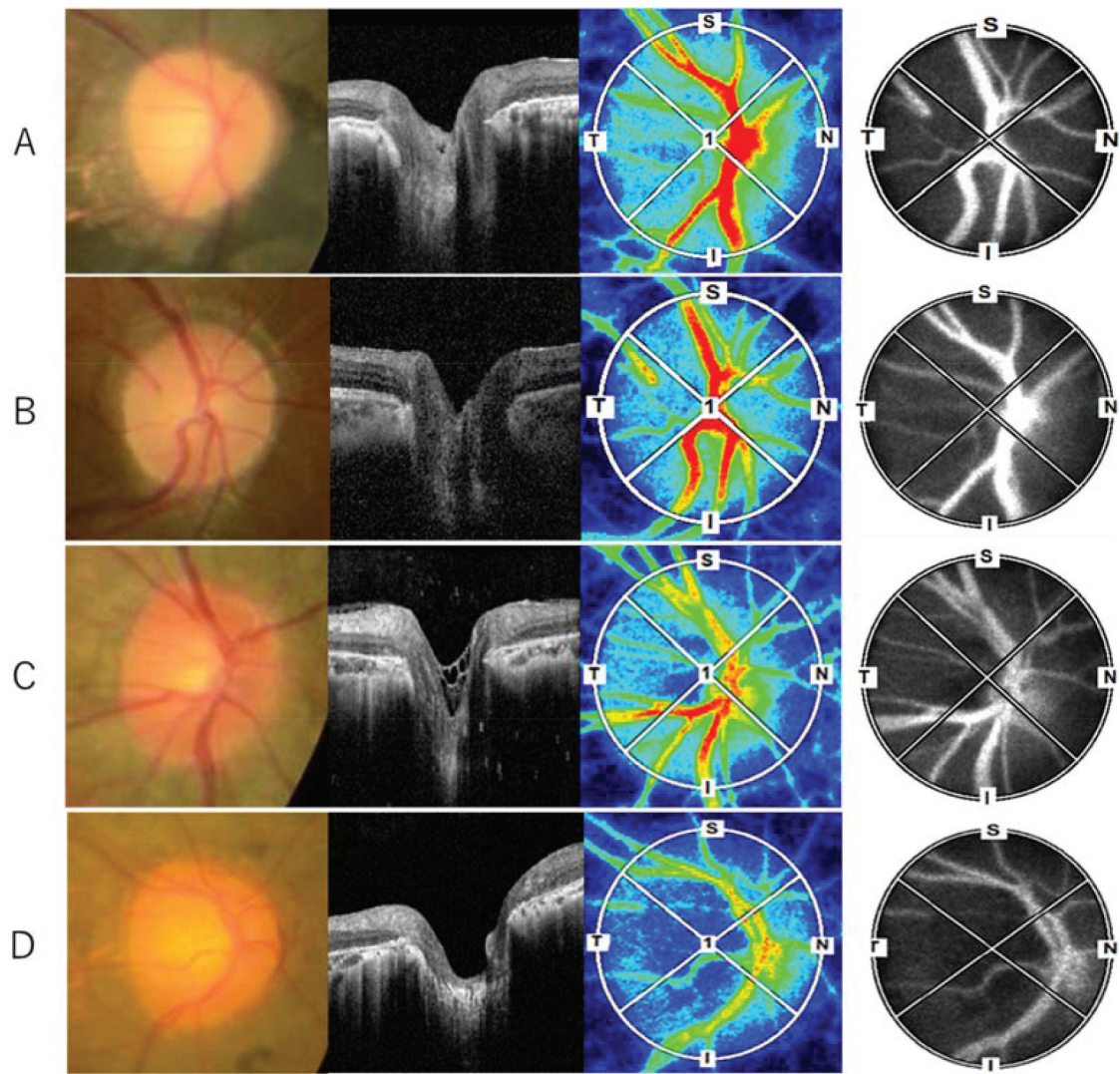


Figure 2. Representative ONH of RP patients with (A, B) and without (C, D) waxy pallor appearance of the ONH, and with (A, C) and without (B, D) a hyper-reflective structure on the ONH. ONH, optic nerve head; RP, retinitis pigmentosa.

Table 2. The correlation between a pale appearance and the presence of a hyper-reflective structure.

	Pale	Not pale	Total
Presence of a hyper-reflective structure	1	6	7
Did not exist	9	12	21
Total	10	18	28

A pale ONH was noted in 10 (35%) out of 28 eyes, and seven (25%) out of 28 eyes had hyper-reflective structures on the ONH based on OCT volume slices (Table 2). However, we did not find a significant correlation between the pale appearance and the presence of a hyper-reflective tissue (Pearson's chi-squared test, $p = .364$).

The MA, MT, and MV of RP patients were 8.65 ± 3.08 AU, 17.81 ± 7.54 AU, and 6.4 ± 2.66 AU, respectively. Figure 3 shows the MT and MV of patients with and without a pale ONH. The MBR was significantly decreased in patients with and without a pale ONH (MV, 11.69 ± 3.32 AU versus 21.22 ± 7.31 AU, respectively, $p < .05$; MT, 4.31 ± 1.00 AU versus 7.56 ± 2.67 AU, respectively, $p < .05$).

The global RNFL thickness of the RP patients was $73.54 \pm 18.82 \mu\text{m}$. Figure 4 shows the quadrant and global measurement of RNFL thicknesses of RP patients with and without a pale ONH in the OCT analysis. The mean nasal quadrant RNFL thickness was $45.53 \pm 25.49 \mu\text{m}$; the mean temporal quadrant RNFL thickness was $81.89 \pm 19.67 \mu\text{m}$; the mean

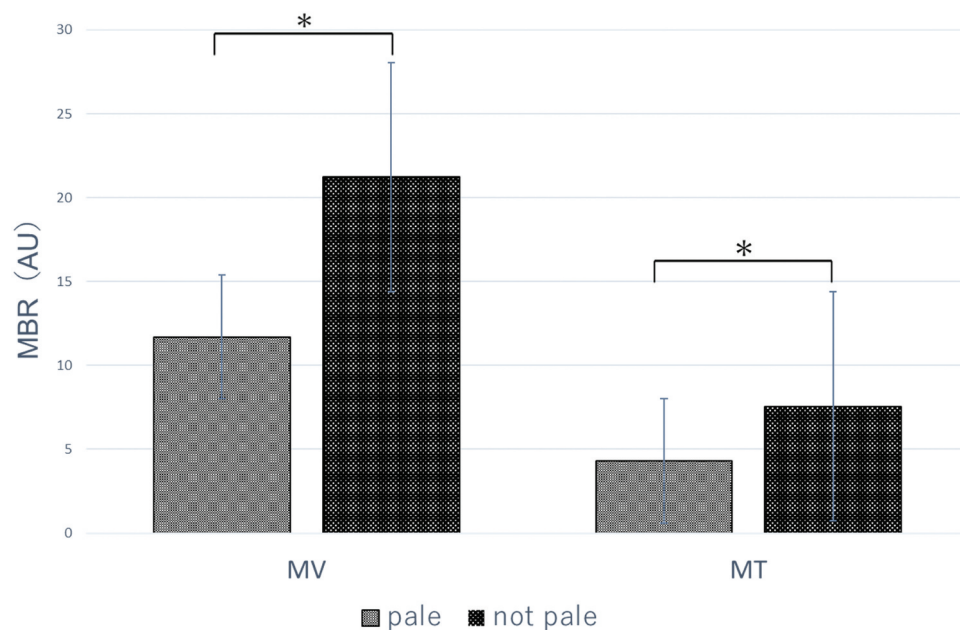


Figure 3. LSFG parameters (MV, MT) with and without a pale ONH. LSFG, laser speckle flowgraphy; MV, optic nerve head vessel area; MT, optic nerve head tissue area; ONH, optic nerve head; MBR, mean blur rate.

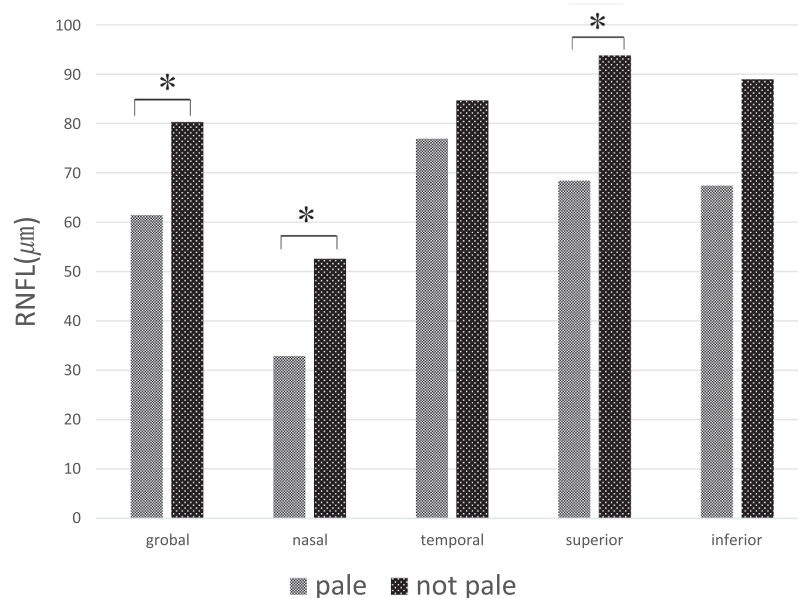


Figure 4. RNFL thickness divided into four quadrants with and without a pale ONH. RNFL, retinal nerve fiber layer; ONH, optic nerve head.

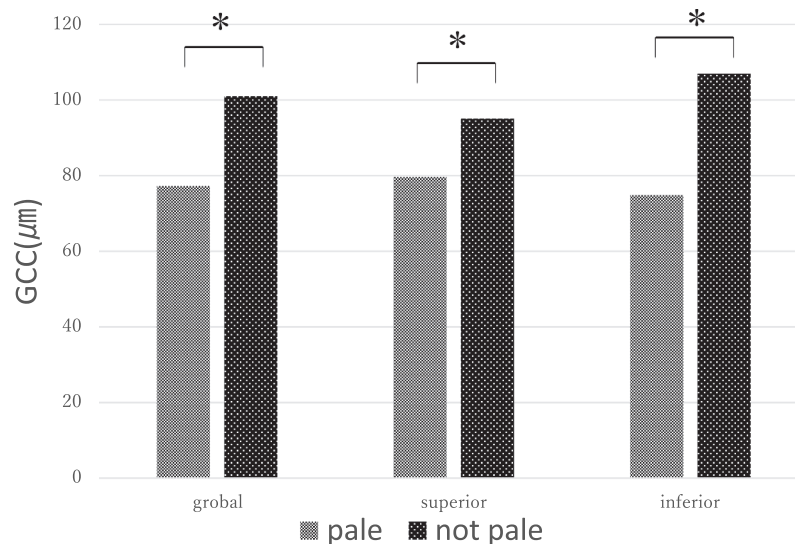


Figure 5. GCC thickness divided into two quadrants with and without a pale ONH. GCC, ganglion cell complex; ONH, optic nerve head.

superior quadrant RNFL thickness was $84.71 \pm 23.79 \mu\text{m}$; and the mean inferior quadrant RNFL thickness was $81.25 \pm 26.38 \mu\text{m}$. There were significant differences observed between patients with and without a pale ONH in the nasal quadrant ($32.9 \pm 15.05 \mu\text{m}$ versus $52.5 \pm 28.36 \mu\text{m}$, respectively, $p < .05$), superior quadrant ($68.40 \pm 20.51 \mu\text{m}$ versus $93.77 \pm 21.58 \mu\text{m}$, respectively, $p < .05$), and global measurements ($61.4 \pm 17.4 \mu\text{m}$ versus $80.29 \pm 16.95 \mu\text{m}$, respectively, $p < .05$). However, no significant differences were observed in the temporal ($p = .472$) and inferior ($p = .108$) quadrants.

Figure 5 shows the quadrant and global measurement of GCC thicknesses of RP patients with and without a pale ONH in the OCT analysis. The global GCC thickness was $93.17 \pm 30.84 \mu\text{m}$; the mean superior quadrant GCC thickness was $89.55 \pm 17.26 \mu\text{m}$; and the mean inferior quadrant GCC thickness was $95.50 \pm 52.41 \mu\text{m}$. There were significant differences observed between patients with and without a pale ONH in the superior quadrant ($79.62 \pm 18.16 \mu\text{m}$ versus $95.06 \pm 13.97 \mu\text{m}$, respectively, $p < .05$), inferior quadrant ($74.85 \pm 19.83 \mu\text{m}$ versus $106.98 \pm 60.71 \mu\text{m}$, respectively, $p < .05$), and global measurements ($77.23 \pm 18.69 \mu\text{m}$ versus $101.02 \pm 32.91 \mu\text{m}$, respectively, $p < .05$).

DISCUSSION

This study assessed changes in the color, blood flow, and structure of the ONH in patients with RP by using fundus photography, LSFG, and OCT. Our findings suggest that both the RNFL and blood flow in the ONH were attenuated in patients with RP, wherein a trend of further decrease in patients with pallor of the ONH was observed. These results indicate that the pale appearance of the ONH in patients with RP is clinically significant.

Several hypotheses have been proposed for the waxy pallor appearance of the ONH. The first theory was based on pathological findings and described the formation of astrocytic gliosis and the migration and proliferation of connective tissue in the ONH.⁷ Gliosis is the neuroprotective response of the macroglia (astrocytes and Müller cells) to pathogenic stimuli and is

a hallmark of several neurodegenerative diseases of the retina.¹¹ In 2016, Saba et al. clinically measured this preretinal membrane using OCT and found that RP had glial membrane-like structures on the ONH surface in 55.1% of RP patients and that the ONH pallor and prelaminar structures were correlated.¹² However, the relationship between glial formation and the progression of atrophy is not conclusive because the preretinal membrane does not exist in the exact region where photoreceptor degeneration has progressed, such as the ONH.¹³

We investigated the ONH using a vertical slice of OCT and were able to confirm hyper-reflective structures in 25% of patients; however, no relationship with ONH pallor was observed. There are several possible reasons for this discrepancy. The small number of studies included only Japanese subjects, and the color tone of the melanin-rich ocular fundus may also affect the evaluation of ONH pallor. We also found hyper-reflective structures on the ONH in patients with RP, and their clinical significance needs to be further investigated in the future.

The second hypothesis is that decreased blood flow affects the natural pink-reddish contrast of the ONH. Recently, several studies using various devices have described the role of vascular dysfunction in RP progression. Color Doppler imaging (CDI) and spectral flow color Doppler sonography, which can measure absolute velocities, showed attenuated blood flow in the central retinal and posterior ciliary arteries in patients with RP.^{14–16} OCT angiography is a convenient, non-invasive technique that can visualize blood vessels with constant blood flow, wherein a decrease in the vessel density of the radial peripapillary capillary network in RP patients has been reported.¹⁷ The LSFG is a clinically convenient and non-invasive device for measuring blood flow. A direct comparison between the hydrogen gas clearance method⁹ and the microsphere method¹⁸ showed that the MBR value represents blood flow. Murakami et al. performed LSFG in patients with RP and showed that the macular MBR, which could indicate choroidal blood flow from the short posterior ciliary arteries and veins, was decreased. The decrease in MBR was significantly associated with reductions in visual acuity, retinal sensitivity, central foveal thickness, and EZ width.¹⁹

This study is the first to show a decrease in the blood flow to the ONH in RP using LSFG. This decrease in blood flow was consistent with the results of the CDI evaluation.^{14,15} In the present study, we investigated the change in blood flow to the MV and MT. The MV reflects blood flow in the major retinal vessels supplied by the central retinal artery and vein, while the MT reflects blood flow in the ONH peripheral circulation supplied by the short posterior ciliary artery and vein.²⁰ We found that both MT and MV were decreased, compared with past reports of normal subject data with similar average age.^{21,22} Direct analysis that distinguishes the retinal flow and short posterior ciliary artery would lead to a better evaluation of the pathology. We found that the blood flow in both the MT and MV in patients with a pale ONH was significantly decreased compared with that in patients without a pale ONH. However, the direct relationship between decreased blood flow and a pale ONH could not be investigated in this study protocol, and further studies with a larger number of patients are required.

The third hypothesis is that atrophy of the RNFL causes a pale appearance of the ONH. The RNFL was affected as the second change, beginning with the loss of neuronal input to the ganglion cells due to the death of the photoreceptor cells.²³ Histological studies have reported a decrease in the number of ganglion cells in RP compared to that in normal populations.²⁴ However, the conclusions of *in vivo* studies using OCT were not unanimous; Walia et al. reported RNFL thinning in approximately 40% of RP patients using SD-OCT,²⁵ and Oishi et al. reported no significant difference between RNFL thickness in normal populations and RP patients using time domain OCT.²⁶ Yildirim et al. reported that 48% of patients had temporal quadrant RNFL thickening and suggested that glial tissue proliferation, which is secondary to the nerve fiber layer atrophy or edema of the remnant RNFL, causes the retinal thickening.²⁷ These results indicate that RNFL thinning may not be linear and may vary from one stage to another of degeneration.

In our study, we found that the RNFL tended to be thin, especially on the nasal side, which is consistent with histopathological reports, suggesting the degeneration on the nasal side of patients with RP.²⁸ Moreover, we found that the RNFL was thinner in patients with a pale ONH, which is consistent with previous reports. Walia et al. observed RNFL deficiency in RP and found RNFL deficiency in seven of seven eyes (100%) with moderate to severe pallor of the ONH and in 16 of 63 eyes (25%) with normal-mild pallor of the ONH. Prospective studies are required to determine the causal relationship between the pallor of the ONH and RNFL defects.

Moreover, we investigated the relationship between GCC thickness and pallor of the ONH. We found that the GCC was also significantly thinner in patients with a pale ONH, which is consistent with previous studies. GCC thickness was reported to be thinner in RP patients compared to healthy subjects.^{29,30} This result demonstrates the relationship between RNFL and the ONH atrophy.

This study had several limitations. The number of cases was small, and multivariate analysis was not possible; therefore, this study was an exploratory research, and the factors that contributed the most to the waxy pallor of the ONH could not

be statistically examined. Additionally, we only included Japanese patients who did not undergo genetic analysis. To eliminate this subjective factor in evaluating the ONH color tone, three doctors, a retinal specialist, and a glaucoma specialist, made independent judgments. However, we included a mixture of eyes with mild cataracts and intraocular lenses, which may have affected the color tone of the optic disc in fundus photographs.

In conclusion, this cross-sectional multimodal observational study demonstrated a decrease in RNFL thickness and blood flow in the ONH of patients with RP, and this tendency was particularly obvious in the ONH with pallor. In photoreceptor cell transplantation and gene therapy, the condition of secondary neurons and beyond is a factor that influences the therapeutic effect; therefore, a multifaceted evaluation of the ONH is required.

ABBREVIATIONS

RP	Retinitis pigmentosa
ONH	Optic nerve head
OCT	Optical coherence tomography
RNFL	Retinal nerve fiber layers
GCC	Ganglion cell complex
LSFG	Laser speckle flowgraphy
SE	Spherical equivalent
BCVA	Best-corrected visual acuity
logMAR	Logarithm of the minimum angle of resolution
SD-OCT	Spectral-domain optical coherence tomography
EZ	Ellipsoid zone
MBR	Mean blur rate
AU	Arbitrary units
MA	Optic nerve head area
MV	Optic nerve head vessel area
MT	Optic nerve head tissue area
SBP	Systolic blood pressure
DBP	Diastolic blood pressures
MAP	Mean arterial pressure
CDI	Color Doppler imaging

ACKNOWLEDGMENTS

The authors thank Dr. Takumi and Dr. Shun Kumashiro for grading the ONH as pale or non-pale using fundus photographs. We also thank Akihiko Kumasaka (Stagen) for providing us with the statistics.

FUNDING

The author(s) reported there is no funding associated with the work featured in this article.

DISCLOSURE STATEMENT

No potential conflict of interest was reported by the author(s).

ETHICS APPROVAL AND CONSENT TO PARTICIPATE

This prospective study adhered to the principles of the Declaration of Helsinki and was approved by the ethics committee of the Toho University Omori Medical Center (approval number: M20053). All participating patients provided informed consent to participate in this observational study.

AVAILABILITY OF DATA AND MATERIALS

The datasets used and/or analyzed during the current study are available from the corresponding author upon reasonable request.

REFERENCES

- Hartong DT, Berson EL, Dryja TP. Retinitis pigmentosa. *Lancet*. 2006;368(9549):1795–1809. doi:10.1016/S0140-6736(06)69740-7.
- Berson EL. Retinitis pigmentosa. The Friedenwald lecture. *Invest Ophthalmol Vis Sci*. 1993;34(5):1659–1676.
- Lu LJ, Liu J, Adelman RA. Novel therapeutics for stargardt disease. *Graefes Arch Clin Exp Ophthalmol*. 2017;255:1057–1062. doi:10.1007/s00417-017-3619-8.
- Mandai M, Watanabe A, Kurimoto Y, Hirami Y, Morinaga C, Daimon T. Autologous induced stem-cell-derived retinal cells for macular degeneration. *N Engl J Med*. 2017;376(11):1038–1046. doi:10.1056/NEJMoa1608368.
- Humayun MS, Dorn JD, Da Cruz L, Dagnelie G, Sahel JA, Stanga PE. Interim results from the international trial of second sight's visual prosthesis. *Ophthalmology*. 2012;119(4):779–788. doi:10.1016/j.ophtha.2011.09.028.
- Bhatti MT. Retinitis pigmentosa, pigmentary retinopathies, and neurologic diseases. *Curr Neurol Neurosci Rep*. 2006;6:403–413. doi:10.1007/s11910-996-0021-z.
- Milam AH, Li ZY, Fariss RN. Histopathology of the human retina in retinitis pigmentosa. *Prog Retin Eye Res*. 1998;17(2):175–205. doi:10.1016/s1350-9462(97)00012-8.s.
- Walia S, Fishman GA. Retinal nerve fiber layer analysis in RP patients using Fourier-domain OCT. *Invest Ophthalmol Vis Sci*. 2008;49:3525–3528. doi:10.1167/iops.08-1842.
- Sugiyama T, Araie M, Riva CE, Schmetterer L, Orgul S. Use of laser speckle flowgraphy in ocular blood flow research. *Acta Ophthalmol*. 2010;88(7):723–729. doi:10.1111/j.1755-3768.2009.01586.x.
- Kanda Y. Investigation of the freely available easy-to-use software 'EZ' for medical statistics. *Bone Marrow Transplant*. 2013;48(3):452–458. doi:10.1038/bmt.2012.244.
- Roche SL, Ruiz-Lopez AM, Moloney JN, Byrne AM, Cotter TG. Microglial-induced müller cell gliosis is attenuated by progesterone in a mouse model of retinitis pigmentosa. *Glia*. 2018;66:295–310. doi:10.1002/glia.23243.
- Al Rashaed S, Khan AO, Nowilaty SR, Edward DP, Kozak I. Spectral-domain optical coherence tomography reveals prelamellar membranes in optic nerve head pallor in eyes with retinitis pigmentosa. *Graefes Arch Clin Exp Ophthalmol*. 2016;254:77–81. doi:10.1007/s00417-015-3015-1.
- Szamier RB. Ultrastructure of the preretinal membrane in retinitis pigmentosa. *Invest Ophthalmol Vis Sci*. 1981;1(4):227–236. doi:10.1097/00006982-198101040-00009.
- Taner P, Kara SA, Akarsu C, Ergin A. The effects of darkness on reticulobar hemodynamics in patients with early stages retinitis pigmentosa. *Int Ophthalmol*. 2004;25:95–99. doi:10.1023/b:inte.0000031743.67336.b5.
- Kiseleva TN, Zol'nikova D IV, Ramazanova ON, Egorova KA, Rogatina EV. Ocular blood flow and retinal electrogenesis in retinitis pigmentosa. *Vestn Oftalmol*. 2015;131(5):14–19. doi:10.17116/oftalma2015131514-19.
- Cellini M, Lodi R, Possati GL, Sbrocca M, Pelle D, Giubilei N. Echo-Doppler couleur dans la rétinopathie pigmentaire. Etude préliminaire [Color Doppler ultrasonography in retinitis pigmentosa. Preliminary study]. *J Fr Ophtalmol*. 1997;20(4):659–663. doi:10.1007/BF00175262.
- Mastropasqua R, Borrelli E, Agnifili L, Toto L, Antonio Di L, Senatore A. Radial peripapillary capillary network in patients with retinitis pigmentosa: an optical coherence tomography angiography study. *Front Neurol*. 2017;8:572. doi:10.3389/fneur.2017.00572.
- Tamaki Y, Araie M, Kawamoto E, Eguchi S, Fujii H. Noncontact, two-dimensional measurement of retinal microcirculation using laser speckle phenomenon. *Invest Ophthalmol Vis Sci*. 1994;35(11):3825–3834.
- Murakami Y, Funatsu J, Nakatake S, Fujiwara K, Tachibana T, Koyanagi Y. Relations among foveal blood flow, retinal-choroidal structure, and visual function in retinitis pigmentosa. *Invest Ophthalmol Vis Sci*. 2018;59:1134–1143. doi:10.1167/iops.17-23050.
- Enomoto N, Anraku A, Tomita G, Iwase A, Sato T, Shoji N. Characterization of laser speckle flowgraphy pulse waveform parameters for the evaluation of the optic nerve head and retinal circulation. *Sci Rep*. 2021;11:6847. doi:10.1038/s41598-021-86280-5.
- Aizawa N, Kunikata H, Nitta F, Shiga Y, Omodaka K, Tsuda S. age- and sex-dependency of laser speckle flowgraphy measurements of optic nerve vessel microcirculation. *PLOS ONE*. 2016;11(2):e0148812. doi:10.1371/journal.pone.0148812.
- Luft N, Wozniak PA, Aschinger GC, Fondi K, Bata AM, Werkmeister RM. Ocular blood flow measurements in healthy white subjects using laser speckle flowgraphy. *PLoS One*. 2016;11(12):e0168190. doi:10.1371/journal.pone.0168190.
- Stone JL, Barlow WE, Humayun MS, De Juan E, Milam AH. Morphometric analysis of macular photoreceptors and ganglion cells in retinas with retinitis pigmentosa. *Arch Ophthalmol*. 1992;110(11):1634–1639. doi:10.1001/archophth.1992.01080230134038.
- Eng JG, Agrawal RN, Tozer KR, Ross-Cisneros FN, Dagnelie G, Greenberg RJ. Morphometric analysis of optic nerves and retina from an end-stage retinitis pigmentosa patient with an implanted active epiretinal array. *Invest Ophthalmol Vis Sci*. 2011;52:4610–4616. doi:10.1167/iops.09-4936.
- Walia S, Fishman GA, Edward DP, Lindeman M. Retinal nerve fiber layer defects in RP patients. *Invest Ophthalmol Vis Sci*. 2007;48:4748–4752. doi:10.1167/iops.07-0404.
- Oishi A, Otani A, Sasahara M, Kurimoto M, Nakamura H, Kojima H. Retinal nerve fiber layer thickness in patients with retinitis pigmentosa. *Eye (Lond)*. 2009;23:561–566. doi:10.1038/eye.2008.63.
- Yıldırım MA, Erden B, Tetikoğlu M, Kuru Ö, Elçioğlu M. Analysis of the retinal nerve fiber layer in retinitis pigmentosa using optical coherence tomography. *J Ophthalmol*. 2015;2015:157365. doi:10.1155/2015/157365.
- Flannery JG, Farber DD, Bird AC, Bok D. Degenerative changes in a retina affected with autosomal dominant retinitis pigmentosa. *Invest Ophthalmol Vis Sci*. 1989;30(2):191–211.
- Toto L, Borrelli E, Mastropasqua R, Senatore A, Di Antonio L, Di Nicola M. Macular features in retinitis pigmentosa: correlations among ganglion cell complex thickness, capillary density, and macular function. *Invest Ophthalmol Vis Sci*. 2016;57:6360–6366. doi:10.1167/iops.16-20544.
- Hideki F, Tomoyuki H, Shigeru K. Utility of evaluating ganglion cell complex thickness for retinitis pigmentosa. *J Eye*. 2016;33:151–154.